Electromagnetically induced transparency using a vapor cell and a laser-cooled sample of cesium atoms

Jason J. Clarke and William A. van Wijngaarden*
Physics Department, Petrie Building, York University, 4700 Keele Street, Toronto, Ontario, Canada M3J 1P3

Hongxin Chen
EXFO Electro-Optical Engineering, 465 Avenue Godin Vanier, Quebec, Quebec, Canada G1M 3G7
(Received 12 February 2001; published 18 July 2001)

Electromagnetically induced transparency (EIT) was observed in a mismatched-wavelength cascade system using a room temperature vapor cell and laser-cooled atoms. A cw probe laser beam monitored the cesium $6S_{1/2}\rightarrow 6P_{3/2}$ transition while another cw laser coupled the $6P_{3/2}$ state to a higher excited state. The ratio of the observed Rabi frequencies for coupling to the $6P_{3/2}\rightarrow(11-13)D_{3/2,5/2}$ transitions agreed closely with that predicted using the transition oscillator strengths. A comparison of the EIT signals obtained using cold atoms and the vapor cell is made.

DOI: 10.1103/PhysRevA.64.023818 PACS number(s): 42.50.Gy, 32.80.Pj, 32.70.Cs

I. INTRODUCTION

Electromagnetically induced transparency or EIT is a quantum interference effect that occurs when a weak probe light field in resonance with an atomic transition propagates through a medium with reduced absorption due to the effect of a strong coupling light field on a linked transition. The three levels involved can be in cascade, Λ, or V configurations [1–7]. EIT has numerous applications and was recently used to slow [8,9] and even stop light [10].

EIT was first observed using a high-power pulsed laser that interacted with a strontium vapor in a Λ system [11,12]. EIT has since been studied with cw lasers in various media including solids [13,14], vapor cells [15–23], atomic beams [24], and recently laser-cooled atoms [25–34], and even Bose Einstein condensates [8,9]. EIT in three- and four-level systems has also been shown to have applications in nonlinear optics such as four-wave mixing [35,36]. Lasing without inversion has been demonstrated for systems with mismatched wavelengths [23,24]. Several groups have also proposed optical switches and wavelength converters based on EIT for the telecommunications industry [37–39].

EIT is generated using a laser beam that couples two atomic states $|2\rangle$ and $|3\rangle$. This shifts the energies of the states resulting in the Autler-Townes splitting given by the Rabi frequency

$$\Omega=\frac{e\langle r\rangle E}{\hbar} \tag{1}$$

where e is the electron charge, $\langle r\rangle$ is the expectation value of the valence electron position relative to the nucleus, E is the magnitude of the coupling laser electric field, and $\hbar$ is Planck's constant. EIT signals are obtained using a second probe laser that scans across a transition linking state $|2\rangle$ to another state $|1\rangle$. The absorption of an atomic vapor is therefore expected to decrease if the Rabi frequency exceeds the Doppler width $\Delta\omega_D$. However, it has been shown by solving the density matrix describing the atomic system in the presence of the laser fields that EIT occurs when the following less restrictive condition is met [16]:

$$\frac{\Omega^2}{\gamma\Delta\omega_D}\gg 1 \tag{2}$$

where $\gamma=(\Gamma_1+\Gamma_3)/2$ and Γ_1 and Γ_3 are the linewidths of states $|1\rangle$ and $|3\rangle$. In our case $|1\rangle$ is the ground state and $|3\rangle$ is a low-lying excited S or D state resulting in $\gamma\approx 0.25$ MHz. For a thermal vapor of alkali-metal atoms, $\Delta\omega_D\approx 500$ MHz and Eq. (2) is satisfied if $\Omega>10$ MHz. Such Rabi frequencies are readily obtained using focused cw laser beams.

It was recently shown that the EIT signal obtained in a cascade system is significantly larger than that found using Λ or V configurations [21]. Moreover, for a given coupling laser power, the maximum EIT signal is obtained using a probe wavelength λ_p that is longer than the coupling laser wavelength λ_c. This is not surprising because transitions at longer wavelengths have smaller Doppler widths.

A requirement for observing EIT using atoms having a velocity v is

$$\Delta_p=\left(\frac{1}{\lambda_p}\pm\frac{1}{\lambda_c}\right)v-\Delta_c \tag{3}$$

where Δ_p and Δ_c are the detunings of the probe and coupling laser beams from the respective resonances. The plus (minus) sign applies if the probe and coupling laser beams are co- (counter)propagating. The EIT signal is independent of the atomic velocity distribution for counterpropagating laser beams if $\lambda_p=\lambda_c$. It has, however, been shown theoretically and experimentally that the EIT signal is unaffected for small laser detunings from resonance by the atomic velocity distribution in a cascade configuration if the coupling and probe laser beams are counterpropagating and $\lambda_p>\lambda_c$ [16,20–22].

Our group has previously examined EIT on a mismatched cascade system in a rubidium vapor cell [39]. A low-power

*Corresponding author. Email address: wvw@yorku.ca

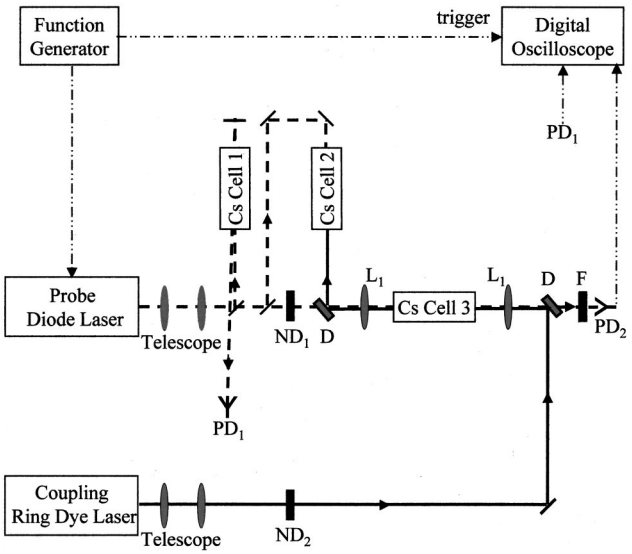

FIG. 1. Apparatus for studying EIT using a cesium vapor cell. See text for a description.

laser diode was scanned across the rubidium $5S_{1/2} \rightarrow 5P_{3/2}$ transition while a higher-power cw dye laser was resonant with a transition from the $5P_{3/2}$ to a higher S or D state. This paper reports EIT observed in a cesium cell where the coupling laser was resonant with a number of transitions connecting the $6P_{3/2}$ state to excited states. This permitted the determination of relative oscillator strengths for the coupling laser transitions.

Laser-cooled atoms provide a preferred medium for studying EIT since collisional dephasing is greatly reduced compared to a thermal vapor. Many of the experiments to date have used the same laser for cooling the atoms and investigating the EIT signal, complicating analysis of the results. In this experiment, atoms were trapped by diode lasers independent of both the probe and coupling lasers used to generate and observe the EIT signal. Hence, the EIT signal could be unambiguously observed. The resulting EIT signals agree with theory and were also compared to those observed in the thermal cesium vapor cell.

II. EIT IN A VAPOR CELL

The apparatus used in this experiment is shown in Fig. 1. Cesium atoms were contained in cylindrical Pyrex vapor cells having a diameter and length of 2.54 cm. The cells were manufactured by attaching them to a vacuum chamber that was pumped down to a pressure of less than 1.0×10^{-6} torr using a diffusion pump and a liquid nitrogen trap. The cell was baked overnight at a temperature of 300 °C to remove impurities. Cesium from an ampoule was then distilled into the cell.

The EIT signals were obtained using a cw broad gain grating stabilized diode laser [ν Focus 6316 Velocity Laser] that served as the probe laser. It generated 13 mW of light having a wavelength between 833 and 853 nm. The manufacturer specified linewidth is less than 1 MHz. The diode laser excited the cesium $6S_{1/2} \rightarrow 6P_{3/2}$ transition at 852 nm as

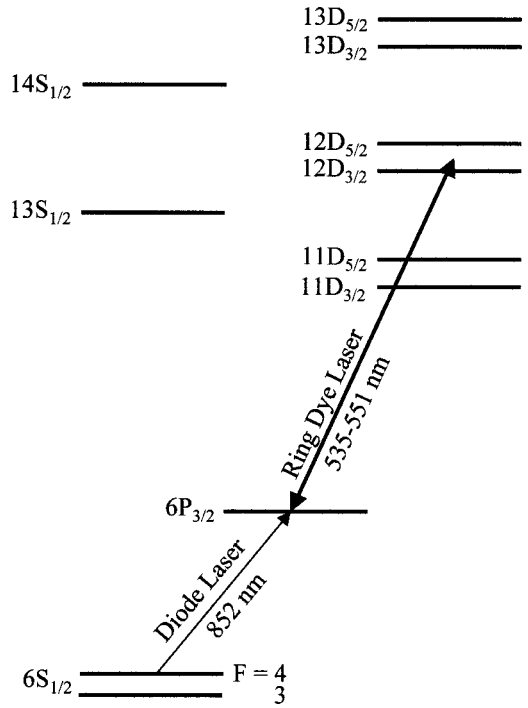

FIG. 2. Low-lying cesium states. The vertical energy axis is not drawn to scale.

is illustrated in Fig. 2. A grating inside the diode laser housing could be adjusted using a piezoelectric crystal to scan the laser frequency across the resonance. The frequency scan was calibrated using a saturation spectroscopy signal [40] observed using Cs cell 1 and a photodiode PD_1. A function generator controlled the laser frequency scan.

The transparency of Cs cell 3 was induced using a cw ring dye laser (Coherent 699) that coupled the $6P_{3/2}$ state to the higher states shown in Fig. 2. The ring laser linewidth is less than 1 MHz and can be tuned over a range of 30 GHz without mode hopping. It generated 500 mW at the transition wavelengths that lie between 535 and 551 nm using pyromethene 556 laser dye. Part of the diode and dye laser beams were directed through a diagnostic cell (Cs cell 2). Fluorescence, produced by the radiative decay of the excited state back to the $6P_{3/2}$ state, was readily visible from this cell, thus ensuring that the ring dye laser wavelength indeed coincided with a particular coupling transition.

The EIT signal was generated by focusing counterpropagating vertically polarized probe diode laser and coupling ring dye laser beams into Cs cell 3. Each laser beam first passed through a telescope that collimated the laser beams in order to facilitate focusing by two separate planoconvex lenses L_1 having a focal length of 10 cm. Cs cell 3 was located midway between the two lenses L_1 that were separated by 20 cm. The diameter of the focused spot sizes of both the diode and dye laser beams was estimated to be 30 μm. The overlap of the two laser beam focal spots was accomplished by optimizing the observed EIT signal. Two calibrated neutral density filters ND_1 and ND_2 were inserted in the laser beam paths to vary the powers of the diode and dye laser beams.

The EIT signal was observed by measuring the transmis-

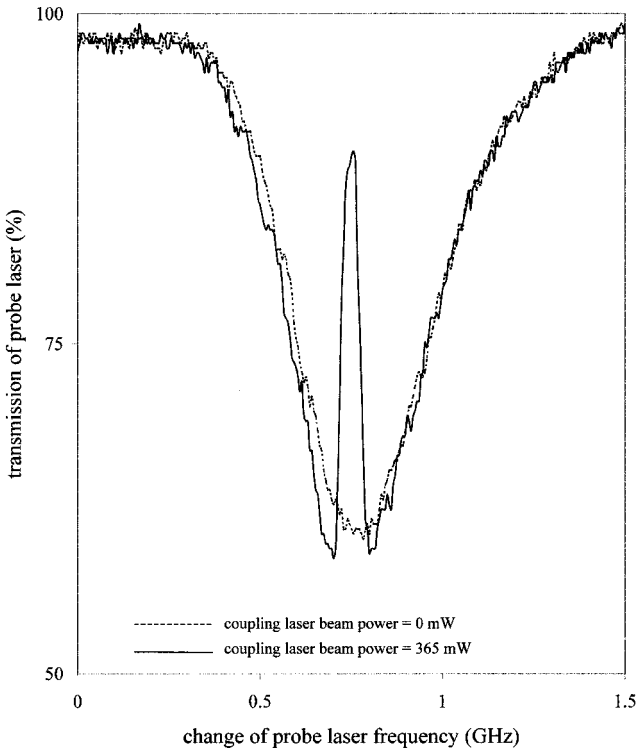

FIG. 3. EIT signal observed in a cesium vapor cell. The diode probe laser was scanned across the $6S_{1/2}(F=4)\rightarrow 6P_{3/2}$ transition while the ring dye laser was resonant with the $6P_{3/2}\rightarrow 11D_{5/2}$ transition.

sion of the diode laser beam through Cs cell 3. The infrared diode laser beam passed through a dielectric mirror D that was transparent to infrared light but reflected the visible coupling laser beam. Residual scattered dye laser light was blocked by a cutoff filter F. A photodiode PD_2 (Thorlabs DET 210) then detected the diode laser beam. The photodiode signal was sent to a digital oscilloscope (Tektronix TDS 3052) that recorded the data.

A diode laser beam power of 20 μW was used to obtain the EIT signals in Cs cell 3. This power optimized the EIT signal, as approximately half of the diode laser power was absorbed when the laser was centered on the $6S_{1/2}(F=4)\rightarrow 6P_{3/2}$ transition. Here, F denotes the hyperfine level. The cell was maintained at room temperature and the corresponding cesium number was estimated to be 1.0×10^{11} atoms/cm^3 [41].

Figure 3 shows the EIT signal where the dashed line corresponds to the Doppler broadened absorption profile observed when the diode laser frequency was scanned over the $6S_{1/2}(F=4)\rightarrow 6P_{3/2}$ transition in the absence of a coupling laser beam [42]. The solid line was obtained using a coupling laser power of 365 mW. The ring dye laser was tuned to the center of the $6P_{3/2}\rightarrow 11D_{5/2}$ transition. The coupling laser beam increased the transmission of the probe diode laser beam through the vapor from 60% to 90%.

Figure 4 shows the effect of detuning the coupling ring dye laser from the center of the $6P_{3/2}\rightarrow 11D_{5/2}$ transition. The frequency where the EIT increases the transmission shifts with the laser detuning as expected. The effect of different coupling laser powers on the EIT signal for the case when the laser is resonant with the $6P_{3/2}\rightarrow 11D_{5/2}$ transition is shown in Fig. 5.

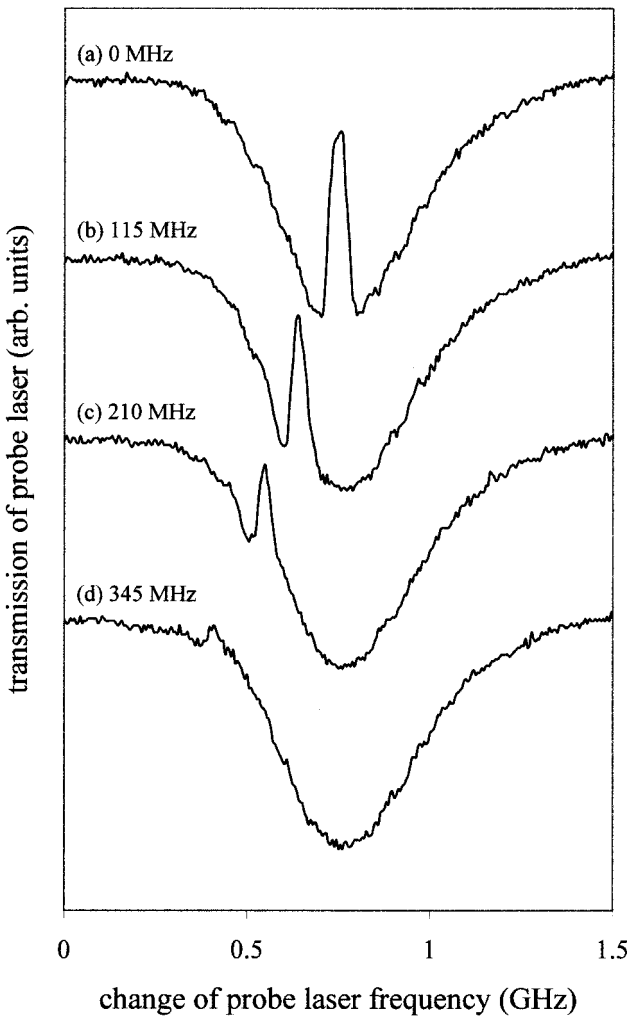

FIG. 4. Effect of detuning the coupling laser. The diode probe laser was scanned across the $6S_{1/2}(F=4)\rightarrow 6P_{3/2}$ transition while the ring dye laser was tuned from the $6P_{3/2}\rightarrow 11D_{5/2}$ transition center by (a) 0 MHz, (b) 115 MHz, (c) 210 MHz, and (d) 345 MHz.

The width of the peaks (full width at minimum transmission of the EIT peak) shown in Fig. 5 is plotted in Fig. 6 versus the square root of the coupling laser beam power. This peak width is a measure of the average Rabi frequency experienced by the atoms that are exposed to a focused coupling laser beam that has a nonuniform spatial profile. The average Rabi frequency at low powers has a larger uncertainty because the EIT signal is smaller than at higher powers. Figure 6 demonstrates that the Rabi frequency depends linearly on the square root of the coupling laser beam power. The width of the EIT peak shows no evidence of broadening due to the Maxwellian velocity distribution of the atoms or other dephasing mechanisms such as the laser linewidth. Similar Doppler-free results have been observed in a cascade configuration using counterpropagating laser beams in a rubidium vapor [20].

Figure 7 shows the EIT signals obtained when the cou-

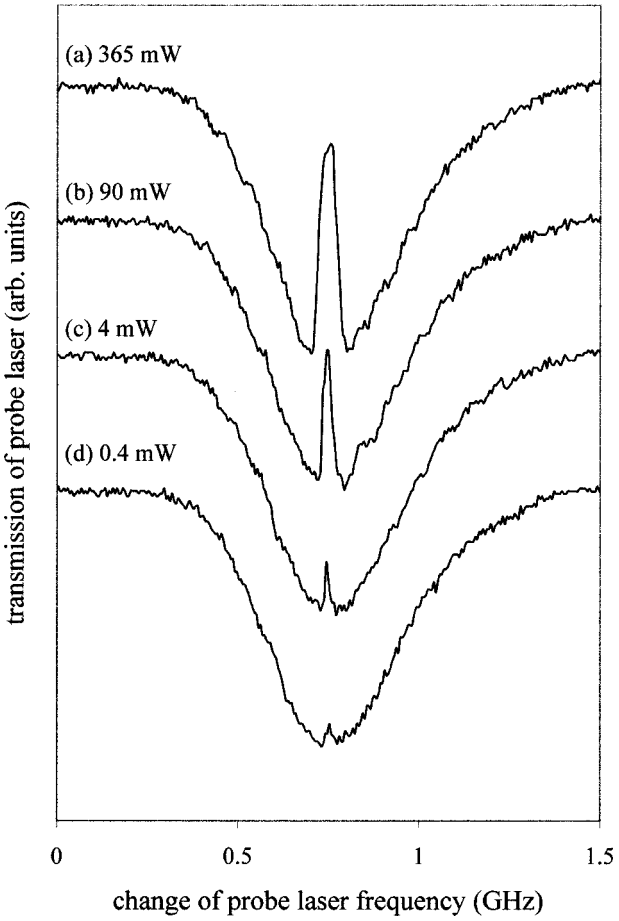

FIG. 5. Effect of various coupling laser powers. The diode probe laser was scanned across the $6S_{1/2}(F=4)\rightarrow 6P_{3/2}$ transition while the power of the ring dye laser resonant with the $6P_{3/2}\rightarrow 11D_{5/2}$ transition was varied as follows: (a) 365 mW, (b) 90 mW, (c) 4 mW, and (d) 0.4 mW.

pling laser frequency is centered on various transitions from the $6P_{3/2}$ state. The Rabi frequency can be expressed as

$$\Omega = \sqrt{KfI} \tag{4}$$

where f is the oscillator strength for the coupling transition, I is the intensity of the coupling laser beam, and K is a constant. For transitions from the $6P_{3/2}$ to the $nD_{3/2,5/2}$ states, the Rabi frequencies and oscillator strengths are related by the following:

$$\frac{\Omega(6P_{3/2}\rightarrow nD_{5/2})}{\Omega(6P_{3/2}\rightarrow nD_{3/2})} = \sqrt{\frac{f(6P_{3/2}\rightarrow nD_{5/2})}{f(6P_{3/2}\rightarrow nD_{3/2})}}. \tag{5}$$

This ratio is predicted to equal 3.0 using computed oscillator strengths [43]. The observed values are 3.1 ± 0.3 when $n=11$,2.9 ± 0.3, when $n=12$, and 2.9 ± 0.3 when $n=13$, in good agreement with the predicted value.

III. EIT IN A MAGNETO-OPTICAL TRAP

Figure 8 shows the apparatus used to investigate EIT in laser-cooled atoms produced by a standard magneto-optical

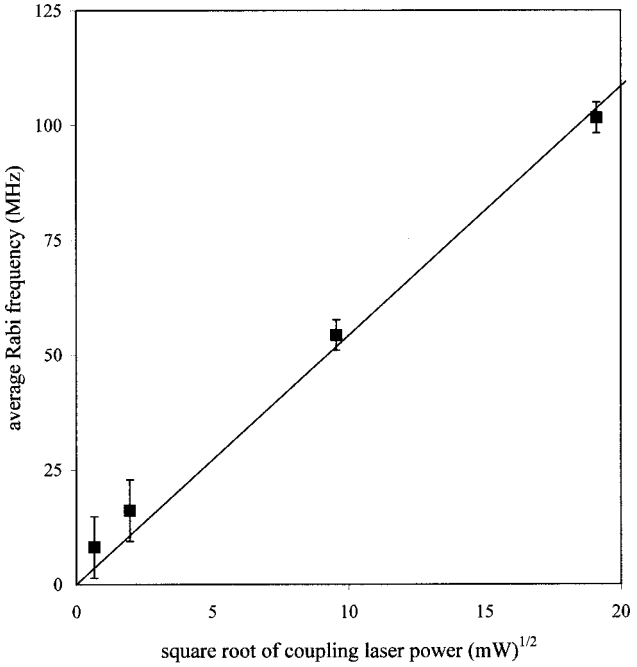

FIG. 6. Dependence of measured Rabi frequency on coupling laser power for the EIT signal observed in a vapor cell.

trap (MOT) [44]. The MOT consisted of a pair of anti-Helmholtz coils having a diameter of 5 cm that generated a magnetic field gradient of 10 G/cm midway between the two coils. Cesium atoms were loaded into the trap from a background vapor that had a pressure of 2×10^{-8} torr. Two diode lasers (Spectra Diode Labs 5712) that generated up to 100 mW of light at 852 nm were used to cool the atoms. The frequency of both diode lasers was stabilized by locking the laser frequency to a cesium transition using saturation absorption spectroscopy. One diode laser called the cooling laser beam was detuned 12 MHz below the $6S_{1/2}(F=4)\rightarrow 6P_{3/2}(F=5)$ transition frequency using an acousto-optic modulator (Brimrose GPF-250-100.852). The cooling laser beam was divided into three pairs of laser beams each having a power of 6 mW counterpropagating along the $\hat{x}$, $\hat{y}$, and $\hat{z}$ directions. The second diode laser, called the repumper laser, excited the $6S_{1/2}(F=3)\rightarrow 6P_{3/2}(F=3 \text{ or } 4)$ transition as illustrated in Fig. 9. The number of cold atoms was estimated using a charge-coupled device camera (SpectraSource Instruments Teleris II) to be 8×10^6 occupying a roughly spherical volume having a radius of 0.5 mm. The temperature of the atoms was estimated to be about 40 μK by measuring the expansion of the cold atom cloud after the MOT was suddenly switched off.

EIT in the laser cooled atoms was observed using the same probe diode and coupling ring dye lasers described previously in Sec. II. These laser beams were vertically polarized and intersected the cold atom cloud at an angle of approximately 5°. The nonzero crossing angle ensured that any observed EIT signal was produced by the cold atoms and not by the thermal background cesium vapor. The ring dye laser beam was first collimated by a telescope and then focused by lens L_2 ($f=50$ cm) to produce a laser beam waist radius of 0.5 mm to overlap the cold atom cloud. The probe

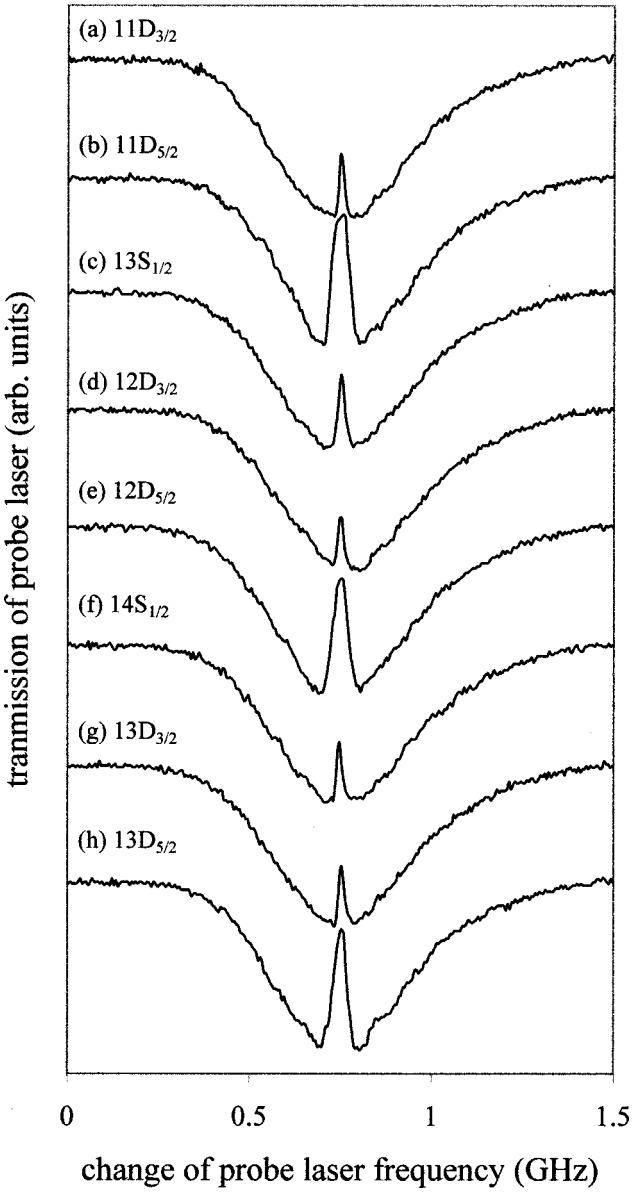

FIG. 7. Effect of different coupling transitions on the EIT signal. The diode probe laser was scanned across the $6S_{1/2}(F=4) \rightarrow 6P_{3/2}$ transition while the ring dye laser coupled the $6P_{3/2}$ state to the (a) $11D_{3/2}$, (b) $11D_{5/2}$, (c) $13S_{1/2}$, (d) $12D_{3/2}$, (e) $12D_{5/2}$, (f) $14S_{1/2}$, (g) $13D_{3/2}$, and (h) $13D_{5/2}$ states.

diode laser beam passed through an aperture A having a radius of 0.5 mm before it intersected the cold atom cloud. The overlap of the probe and coupling laser beams on the cold atom cloud was accomplished by optimizing the observed EIT signal.

The power of the probe diode laser beam that passed through the cold atoms was detected by photodiode PD. The diode laser beam incident on the cold atoms was attenuated to 1 μW using neutral density filter ND_1. This power was selected as too many cold atoms were ejected from the trap using higher probe laser powers while the detected signal became quite small at powers less than 1 μW.

Figure 10 shows signals obtained when (a) the coupling laser was tuned to the $6P_{3/2}(F=4) \rightarrow 11D_{5/2}$ transition while

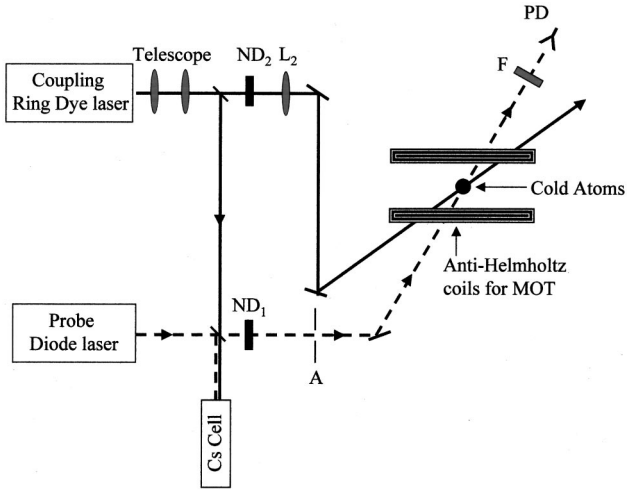

FIG. 8. Apparatus for studying EIT using a MOT. The diode lasers used to generate the cold atoms in the MOT are not shown. See text for a description.

the repumper excited the $6S_{1/2}(F=3) \rightarrow 6P_{3/2}(F=3)$ transition and (b) the coupling laser was tuned to the $6P_{3/2}(F=3) \rightarrow 11D_{5/2}$ transition while the repumper excited the $6S_{1/2}(F=3) \rightarrow 6P_{3/2}(F=4)$ transition. Data were not taken with the coupling laser tuned to excite the $6P_{3/2}(F=5)$ peak as the trap was then emptied of cold atoms. Scans were also taken when the MOT was turned off. All of the scans shown in Figs. 10–12 were obtained by subtracting the data taken when the MOT was off in order to eliminate the effects of the background vapor. The frequency scan was calibrated using the known hyperfine splittings of the $6P_{3/2}$ state.

The EIT signal is shown in Fig. 10(a) by the enhanced transmission when the probe laser is at the center of the $F=4$ peak while in Fig. 10(b) the enhanced transmission is evident when the probe laser is at the center of the $F=3$

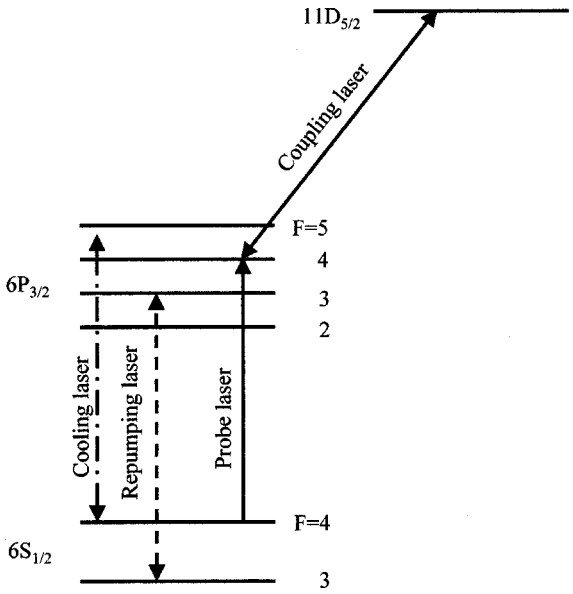

FIG. 9. Relevant energy levels for studying EIT with laser-cooled cesium atoms. The vertical energy axis is not drawn to scale.

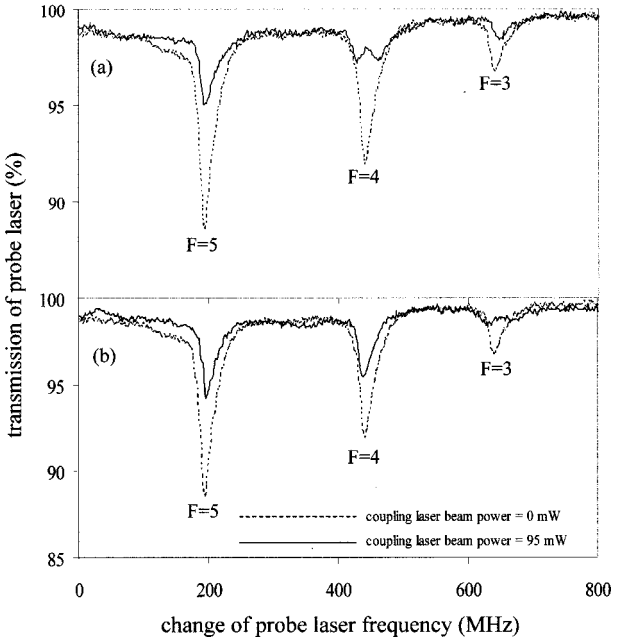

FIG. 10. EIT signal observed in a cesium MOT. The diode probe laser was scanned across the $6S_{1/2}(F=4)\rightarrow 6P_{3/2}(F=3,4,5)$ transitions. The ring dye laser coupled (a) the $6P_{3/2}(F=4)$ level to the $11D_{5/2}$ state while the repumper laser excited the $6S_{1/2}(F=3)\rightarrow 6P_{3/2}(F=3)$ transition and (b) the $6P_{3/2}(F=3)$ level to the $11D_{5/2}$ state while the repumper laser excited the $6S_{1/2}(F=3)\rightarrow 6P_{3/2}(F=4)$ transition.

peak. These scans were taken with the ring dye coupling laser beam attenuated to a power 95 mW using calibrated neutral density filter ND_2. At higher coupling powers the signal was greatly reduced because the number of cold atoms was reduced. Figure 11 shows the characteristic EIT dependence of detuning the coupling ring dye laser from the $6P_{3/2}(F=4)\rightarrow 11D_{5/2}$ transition center. The coupling laser power was 95 mW for the scans at the four different detunings.

Figure 12 examines the dependence of the EIT signal on the power of the coupling ring dye laser beam. All four scans were taken with the coupling laser frequency tuned to the center of the $6P_{3/2}(F=4)\rightarrow 11D_{5/2}$ transition. The power of the coupling laser beam was varied using a calibrated neutral density filter ND_2. The solid lines show fits to the data based on the EIT model developed by Xiao *et al.* [15]. This was done to determine the Rabi frequencies that were then plotted versus the square root of the coupling laser beam power as shown in Fig. 13. An uncertainty of 4 MHz was conservatively estimated for the Rabi frequency due to the fitting accuracy. The data shown in Fig. 13 are consistent with the relationship predicted by Eq. (2).

IV. CONCLUSIONS

Relative oscillator strengths can be determined by comparing the EIT signals generated for different coupling laser transitions. These measurements can be readily made using a vapor cell in which the coupling laser beam is focused. The

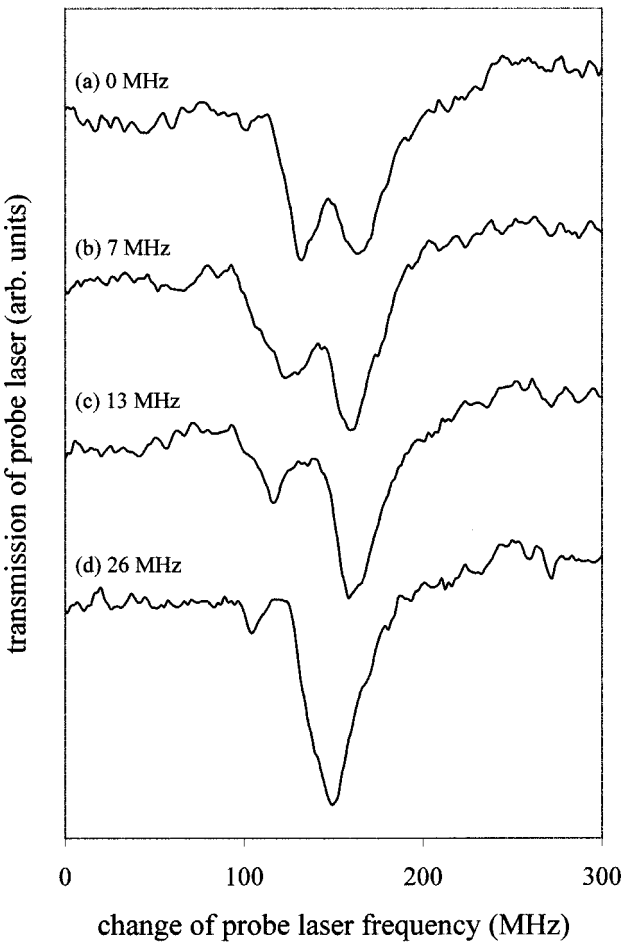

FIG. 11. Effect of detuning the coupling laser. The diode probe laser was scanned across the $6S_{1/2}(F=4)\rightarrow 6P_{3/2}(F=3,4,5)$ transitions while the coupling laser was tuned from the $6P_{3/2}(F=4)\rightarrow 11D_{5/2}$ transition center by (a) 0 MHz, (b) 7 MHz, (c) 13 MHz, and (d) 26 MHz.

width of the EIT signal depends on the square root of the coupling laser beam power and is independent of the Doppler width for a cascade system using counterpropagating beams where $\lambda_p > \lambda_c$. This has also been observed in rubidium atoms by Dunn and co-workers [20–22]. The relative oscillator strengths for the $6P_{3/2}\rightarrow nD_{3/2,5/2}$ transitions where $n=11$–13 were found to agree well with simple theory. Absolute oscillator strengths could be determined knowing the laser intensity of the coupling laser beam. However, the intensity of the focused laser beam varies throughout the cell making it difficult to estimate.

Oscillator strengths are most commonly determined by measuring the absorption of light through a vapor [45]. A significant uncertainty in these measurements is to estimate the atomic number density particularly if a transition between two excited states is considered and the atoms are not in thermal equilibrium. Hence, few reliable oscillator strengths for transitions between excited states exist [46,47]. The method described here is independent of the atomic number density of any state. Information about transition probabilities can also be inferred from measured radiative lifetimes. However, only a handful of lifetimes have been

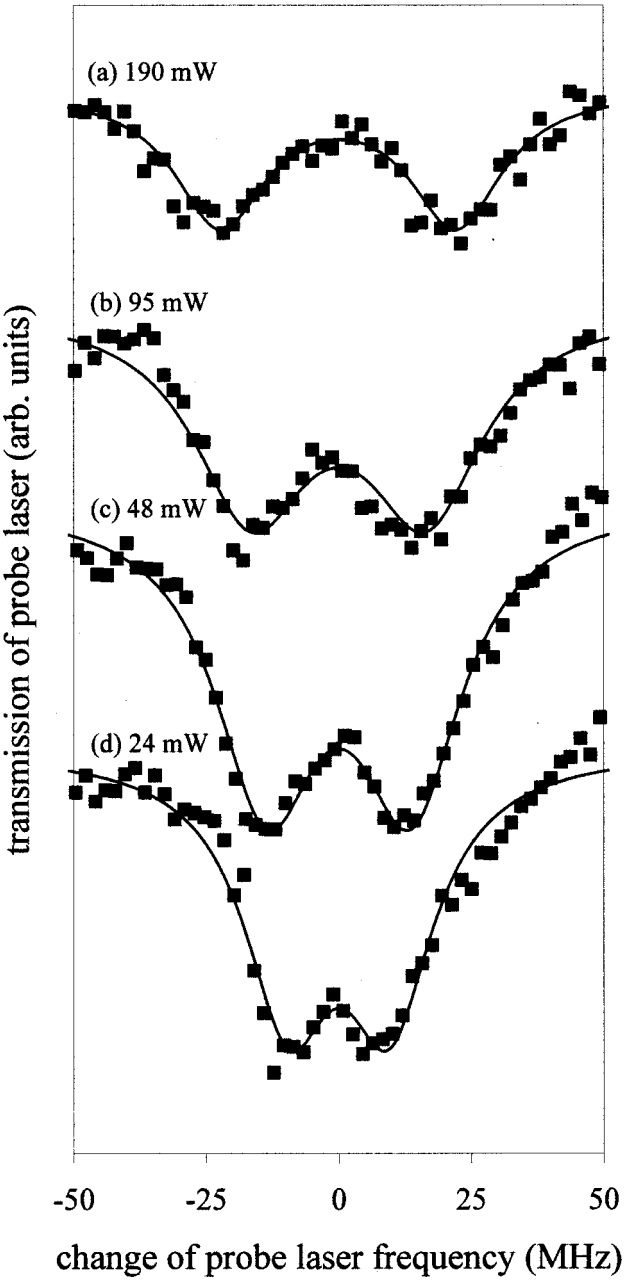

FIG. 12. Effect of changing the coupling laser power. The diode probe laser was scanned across the $6S_{1/2}(F=4)\rightarrow 6P_{3/2}(F=3,4,5)$ transitions while the power of the ring dye laser resonant with the $6P_{3/2}(F=4)\rightarrow 11D_{5/2}$ transition was varied as follows: (a) 190 mW, (b) 95 mW, (c) 48 mW, and (d) 24 mW. The solid line is the theoretical fit to the data as is discussed in the text.

reported in the literature with uncertainties of less than 1%. The present method therefore provides a useful complementary check on the determination of relative transition probabilities.

The maximum observed Rabi frequencies were 102 ± 4 MHz found using the vapor cell (see Fig. 6) and 45 ± 4 MHz obtained using the laser-cooled atoms (see Fig. 13). The Rabi frequency strongly depends on the coupling laser intensity. In the cell, the maximum ring dye coupling laser beam intensity varied from 1×10^2 W/cm^2 at the cell

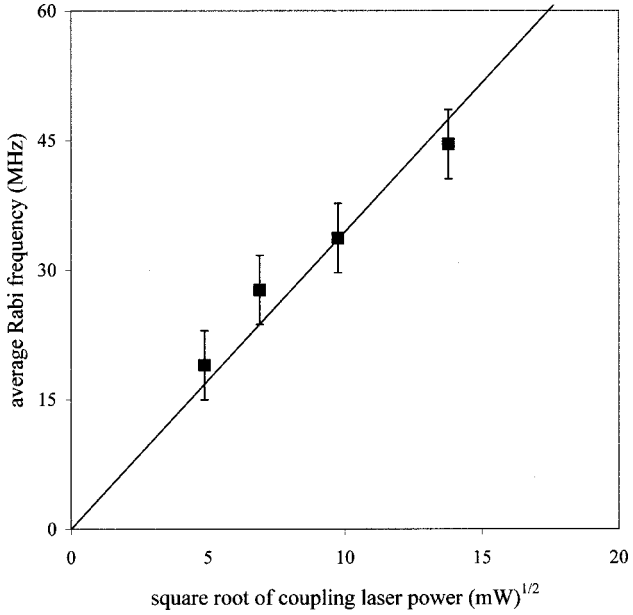

FIG. 13. Dependence of measured rabi frequency on coupling laser power for EIT observed in a MOT.

window to approximately 5×10^4 W/cm^2 at the focus midway in the cell. This compares to a maximum coupling laser intensity of 25 W/cm^2 that was used to illuminate the cold atoms in the MOT. Hence, using Eq. (4) one expects the maximum Rabi frequency in the cell to be larger than that found using the cold atoms by a factor of between 2 and 45. However, comparatively fewer atoms in the vapor cell are at the focus of the coupling laser beam and therefore it is not surprising that the observed ratio of maximum Rabi frequencies observed in the cell and cold atoms is found to be 2.3 ± 0.2.

The advantage of studying EIT using cold atoms as opposed to a vapor cell is that the collision rate is much lower and therefore the rate of dephasing is less. Hence, for a given coupling laser intensity or Rabi frequency, the electromagnetically induced transparency observed using cold atoms is expected to be greater than is found in a vapor cell. Figure 5(b), which corresponds to a Rabi frequency of 54 ± 4 MHz, shows a change in the absorption of the probe laser beam at the line center of 50%. In comparison, Fig. 12(a), which corresponds to a Rabi frequency of 45 ± 4 MHz, shows a change in the absorption profile at the line center of about 75%. Hence, the EIT obtained using cold atoms is greater than the EIT signal observed in a vapor cell obtained using a comparable coupling laser intensity.

In conclusion, EIT is not only an interesting phenomenon with a number of important applications, but can be used to determine quantitative data about atomic transitions.

ACKNOWLEDGMENTS

The authors would like to thank the Natural Science and Engineering Research Council of Canada and the Canadian Institute for Photonic Innovations for financial support. One of us, J.C., acknowledges support from JDS Uniphase.

[1] S.E. Harris, Phys. Today **50** (7), 36 (1997).
[2] J.P. Marangos, J. Mod. Opt. **45**, 471 (1998).
[3] M.O. Scully and M.S. Zubairy, *Quantum Optics* (Cambridge University Press, Cambridge, England, 1997), Chap. 7.
[4] O. Kacharovskaya, Phys. Rep. **219**, 175 (1992).
[5] M.O. Scully, Phys. Rep. **219**, 191 (1992).
[6] P. Mandel, Contemp. Phys. **34**, 235 (1993).
[7] D.J. Fulton *et al.*, Phys. Rev. A **52**, 2302 (1995).
[8] L.V. Hau, S.E. Harris, Z. Dutton, and C.H. Behroozi, Nature (London) **397**, 594 (1999).
[9] S.E. Harris and L.V. Hau, Phys. Rev. Lett. **82**, 4611 (1999).
[10] C. Liu, Z. Dutton, C. Behroozi, and L. Hau, Nature (London) **409**, 490 (2001); D. Phillips, A. Fleischhauer, A. Mair, and R. Walsworth, Phys. Rev. Lett. **86**, 783 (2001).
[11] K.J. Boller, A. Imamoglu, and S.E. Harris, Phys. Rev. Lett. **66**, 2593 (1991).
[12] J.E. Field, K.H. Hahn, and S.E. Harris, Phys. Rev. Lett. **67**, 3062 (1991).
[13] B.S. Ham, S.M. Shahriar, and P.R. Hemmer, J. Opt. Soc. Am. B **16**, 801 (1999).
[14] C. Wie and N.B. Manson, Phys. Rev. A **60**, 2540 (1999).
[15] M. Xiao, Y. Li, S. Jin, and J. Gea–Banacloche, Phys. Rev. Lett. **74**, 666 (1995).
[16] J. Gea-Banacloche, Y. Li, S. Jin, and M. Xiao, Phys. Rev. A **51**, 576 (1995).
[17] Y. Li and M. Xiao, Phys. Rev. A **51**, R2703 (1995).
[18] Y. Li and M. Xiao, Phys. Rev. A **51**, 4959 (1995).
[19] R.R. Moselery *et al.*, Opt. Commun. **119**, 61 (1995).
[20] S. Shepherd, D.J. Fulton, and M.H. Dunn, Phys. Rev. A **54**, 5394 (1996).
[21] J.R. Boon, E. Zekou, D. McGloin, and M.H. Dunn, Phys. Rev. A **59**, 4675 (1999).
[22] J.R. Boon, E. Zekou, D.J. Fulton, and M.H. Dunn, Phys. Rev. A **57**, 1323 (1998).
[23] A.S. Zibrov, M.D. Lukin, D.E. Nikonov, L. Hollberg, M.O. Scully, V.L. Velichansky, and H.G. Robinson, Phys. Rev. Lett. **75**, 1499 (1995).
[24] G.G. Padmabandu, G.R. Welch, I.N. Shubin, E.S. Fry, D.E. Nikonov, M.D. Lukin, and M.O. Scully, Phys. Rev. Lett. **76**, 2053 (1996).
[25] S.A. Hopkins, E. Usadi, H.X. Chen, and A.V. Durrant, Opt. Commun. **138**, 185 (1997).
[26] A.V. Durrant, H.X. Chen, S.A. Hopkins, and J.A. Vaccaro, Opt. Commun. **151**, 136 (1998).
[27] H.X. Chen, A.V. Durrant, J.P. Marangos, and J.A. Vaccaro, Phys. Rev. A **58**, 1545 (1998).
[28] T. van der Veldt, J.F. Roch, P. Grelu, and P. Grangier, Opt. Commun. **137**, 420 (1997).
[29] F.S. Cataliotti, C. Fort, T.W. Hansch, M. Inguscio, and M. Prevedelli, Phys. Rev. A **56**, 2221 (1997).
[30] C. Fort, F.S. Cataliotti, M. Prevedelli, and M. Inguscio, Opt. Lett. **22**, 1107 (1997).
[31] M. Mitsunaga and N. Imoto, Phys. Rev. A **59**, 4773 (1999).
[32] C. Fort, F.S. Cataliotti, T.W. Hansch, M. Inguscio, and M. Prevedelli, Opt. Commun. **139**, 31 (1997).
[33] C.E. Roos, D. Leibfried, A. Mundt, F. Schmidt-Kaler, J. Eschner, and R. Blatt, Phys. Rev. Lett. **85**, 5547 (2000).
[34] M. Muller, F. Homann, R.-H. Rinkleff, A. Wicht, and K. Danzmann, Phys. Rev. A **62**, 060501 (2000).
[35] Y. Li and M. Xiao, Opt. Lett. **21**, 1064 (1996).
[36] J.C. Petch, C.H. Keitel, P.L. Knight, and J.P. Marangos, Phys. Rev. A **53**, 543 (1996).
[37] S.E. Harris and Y. Yamamoto, Phys. Rev. Lett. **81**, 3611 (1998).
[38] H. Schmidt and R.J. Ram, Appl. Phys. Lett. **76**, 3173 (2000).
[39] J.J. Clarke, H.X. Chen, and W.A. van Wijngaarden, Appl. Opt. **40** (12), 2047 (2001).
[40] W. Demtröder, *Laser Spectroscopy*, 2nd ed. (Springer, New York, 1998).
[41] A. Nesmeianov, *Vapour Pressure of the Chemical Elements* (Academic Press, New York, 1963).
[42] The diode laser was also scanned across the $6S_{1/2}(F=3) \rightarrow 6P_{3/2}$ transition and 90% of the beam was transmitted through the cell. This attenuation is lower than when the diode laser excited the $6S_{1/2}(F=4)$ hyperfine level as the subsequent radiative decay of the $6P_{3/2}$ state optically pumps atoms into the $F=4$ ground state hyperfine level where they are no longer in resonance with the laser. The transmission of the probe laser beam increased from 90% to 95% in the presence of a 365 mW coupling ring dye laser beam.
[43] D.R. Bates and A. Damgaard, Philos. Trans. R. Soc. London, Ser. A **242**, 101 (1949); W.A. van Wijngaarden and J. Li, J. Quant. Spectrosc. Radiat. Transf. **52**, 555 (1994).
[44] N. Davis, M.Sc. thesis, York University, 2000.
[45] M. Huber and R. Sandeman, Phys. Scr. **22**, 373 (1980).
[46] W.A. van Wijngaarden, Ph.D. thesis, Princeton University, 1986 (unpublished).
[47] W.A. van Wijngaarden, K.D. Bonin, W. Happer, E. Miron, D. Schreiber, and T. Arisawa, Phys. Rev. Lett. **56**, 2024 (1986).